

Subduction and melting of biogenic and ferromanganese sediments as evidenced by sub-Moho granitoids

Tiago Valim Angelo¹, Christopher J. Spencer¹, Hong-Yan Li², Derek Knaack¹, Ziyi Zhu⁴, Marina Seraine^{1,4}, Nick M. W. Roberts⁵, Evelyne Leduc¹, Sophie Divilek¹, Anna Ren¹, Brian Joy¹, Gui-Mei Lu²

¹Department of Geological Sciences and Geological Engineering, Queen's University, Kingston, ON, K7L 3N6, Canada; ²State Key Laboratory of Deep Earth Processes and Resources, Guangzhou Institute of Geochemistry, Chinese Academy of Sciences, Guangzhou, 510640, China; ³School of Earth, Atmosphere and Environment, Monash University, Melbourne, VIC3168, Australia; ⁴Timescales of Mineral Systems Group, School of Earth & Planetary Science, Curtin University, Perth, WA6845, Australia; ⁵Geochronology and Tracers Facility, British Geological Survey, Nottingham, NG12 5GG, England.

Corresponding author: tiago.angelo@queensu.ca

Supplementary Material A – Additional information for the methods and supplementary figures (SM1 to SM7)

Additional information for the “3. Sampling and analytical methods” section

3.1 Whole-rock Sr-Nd-Pb-Hf isotopes using MC-CP-MS

For Sr-Pb-Hf isotopes, around 50-200 mg of 200 mesh rock powder for each sample was dissolved in an HF-HNO₃ mixture in a Teflon vessel which was heated to 190 °C in an oven for >24 hours. The solution was evaporated to dryness and then added with 1 ml HNO₃ and kept on a hot plate at 140°C for 24 hours. It was then dried down and dissolved in 2.5 M HCl for Sr, 1 M HBr for Pb and 3 M HF for Hf. After centrifugation, the supernatant solution was loaded into an ion-exchange column packed with AG resin for Sr and Pb and LN-Spec resin for Hf. After complete draining, columns were rinsed with 2.5 M HCl for Sr, 1.0 M HBr for Pb, and 3 M HCl, 6 M HCl and 4 M HCl+H₂O₂ (0.5%) for Hf to remove undesirable matrix elements. Finally, the fractions were eluted using 2.5 M HCl for Pb, 6 M HCl for Sr, and 2 M HF for Hf. In the Sr preparation, the residue was

rinsed with 10 ml of 4.0 M HCl and then the REE fraction was eluted using 10 ml of 4.0 HCl. The REE solution was used to separate the Nd fraction by the Nd-column method. The Sr fraction was separated again by the Sr-specific resin. The solution was first converted to the HNO₃ media (3 M HNO₃) and loaded into the Sr-specific resin and pre-conditioned with 6 M HCl and 3 M HNO₃. After draining, columns were rinsed with 3 M HNO₃ to remove undesirable matrix elements. Sr was finally eluted using MQ H₂O and evaporated to dryness prior to mass-spectrometric measurement. For Nd isotopes, the REE solution from the Sr-column method was evaporated to incipient dryness and taken up with 0.18 M HCl. The converted REE solution was loaded into an ion-exchange column packed with LN resin. After draining, columns were rinsed with 0.18 M HCl to remove undesirable matrix elements. The Nd fraction was eluted using 0.3 M HCl and gently evaporated to dryness prior to measurement.

Mass discrimination correction was carried out via normalization to a ⁸⁸Sr/⁸⁶Sr ratio of 8.375209 (Lin et al., 2016), ¹⁴⁶Nd/¹⁴⁴Nd ratio of 0.7219 (Lin et al., 2016), ²⁰⁵Tl/²⁰³Tl ratio of 2.38 (certified value of NIST SRM 997, used for Pb isotopes) and ¹⁷⁹Hf/¹⁷⁷Hf ratio of 0.7325 (Lin et al., 2016). All data reduction for the MC-ICP-MS of the Sr-Nd-Pb-Hf isotope ratios were conducted using “Iso-Compass” software (W. Zhang et al., 2020).

3.2 Hafnium isotopes in zircon using LA-ICPMS

Following a 15-20s period of background analyses, samples were spot ablated for 30s at a 7Hz repetition rate using a 33 μm beam and laser energy of 1.7 J/cm² at the sample surface. The sample cell was flushed by ultrahigh purity He (0.68 L min⁻¹) and N₂ (2.8 mL min⁻¹). Isotopic intensities were measured using an Agilent 7700s quadrupole ICP-MS and a Nu Instruments Plasma II MC-ICP-MS, with high purity Ar as the plasma gas (flow rate 0.98 L min⁻¹). On the quadrupole, half of the split was used for U/Pb dating and published by Spencer et al. (2017). The other half of the split was sent to the MC-ICP-MS for Lu-Hf isotopic measurement. Masses for ¹⁷²Yb, ¹⁷³Yb, ¹⁷⁵Lu, ¹⁷⁶Hf+Yb+Lu, ¹⁷⁷Hf, ¹⁷⁸Hf, ¹⁷⁹Hf and ¹⁸⁰Hf were measured simultaneously.

3.3 Oxygen isotopes in zircon using SIMS

Oxygen isotopes are reported in the conventional delta notation expressed as δ¹⁸O, which reflects the per mil (‰) deviation in the isotope ratio of the sample (¹⁸O/¹⁶O) relative to the Vienna Standard Mean Ocean Water [VSMOW; ¹⁸O/¹⁶O = 205.2 × 10⁻⁶ (Baertschi, 1976)]. ¹⁸O and ¹⁶O ions were detected on Faraday Cup collectors.

Assessing instrumental mass fractionation (IMF) is corrected using the accepted values for the reference materials Laura and 91500. Measured isotopic ratios $(\delta^{18}\text{O}/\delta^{16}\text{O})_{\text{M}}$ are normalized by using the VSMOW, then corrected for IMF using the equations below:

$$(\delta^{18}\text{O})_{\text{M}} = ((\delta^{18}\text{O}/\delta^{16}\text{O})_{\text{M}}/0.0020052 - 1) * 1000 (\text{‰})$$

$$\text{IMF} = (\delta^{18}\text{O})_{\text{M(standard)}} - (\delta^{18}\text{O})_{\text{VSMOW}}$$

$$(\delta^{18}\text{O})_{\text{sample}} = (\delta^{18}\text{O})_{\text{M}} + \text{IMF}$$

3.4 Oxygen isotopes in quartz using IRMS

Oxygen was extracted from approximately 5 mg of each sample, at 550-600 °C, following the conventional bromine pentafluoride (BrF_5) procedure of Clayton and Mayeda (1963) and then measured via dual inlet using a Thermo-Finnigan Delta^{Plus}XP isotope ratio mass spectrometer (IRMS). All oxygen isotopic data in quartz are reported in per mil units (‰) relative to VSMOW. The $\delta^{18}\text{O}$ values are defined as $(R_{\text{sample}} / R_{\text{standard}} - 1) * 1000$, such that $R = {}^{18}\text{O}/{}^{16}\text{O}$.

3.5 Zircon trace element measurements and U-Pb dating by LAICPMS

The analyzed masses were ${}^{31}\text{P}$, ${}^{49}\text{Ti}$, ${}^{89}\text{Y}$, ${}^{91}\text{Zr}$, ${}^{93}\text{Nb}$, ${}^{139}\text{La}$, ${}^{140}\text{Ce}$, ${}^{141}\text{Pr}$, ${}^{146}\text{Nd}$, ${}^{147}\text{Sm}$, ${}^{153}\text{Eu}$, ${}^{157}\text{Gd}$, ${}^{159}\text{Tb}$, ${}^{163}\text{Dy}$, ${}^{165}\text{Ho}$, ${}^{166}\text{Er}$, ${}^{169}\text{Tm}$, ${}^{172}\text{Yb}$, ${}^{175}\text{Lu}$, ${}^{177}\text{Hf}$, ${}^{181}\text{Ta}$, ${}^{206,207,208}\text{Pb}$, ${}^{232}\text{Th}$ and ${}^{238}\text{U}$. Each analysis includes 40-sec of ablation time, using a 28- μm -diameter spot size and a repetition rate of 5 Hz, plus 20-sec pre- and post-ablation background measurements. The analyzed data were processed by Iolite software (Paton et al., 2011), using Si as the internal standard. Zircons with $\text{La} > 1$ ppm or $\text{Ti} > 80$ ppm or $\text{P} > 5000$ ppm were removed from the dataset to exclude samples influenced by inclusions. For zircon grains with ages older than 950 Ma, uncorrected ${}^{207}\text{Pb}/{}^{206}\text{Pb}$ ages were selected as the final age. For younger grains, the age was chosen either an uncorrected ${}^{206}\text{Pb}/{}^{238}\text{U}$ age or a ${}^{207}\text{Pb}$ -corrected ${}^{206}\text{Pb}/{}^{238}\text{U}$ age, depending on which one brought the analysis closer to Concordia. All the selected zircon grains have concordant ages (<5% discordance).

3.6 Lithium isotopes in muscovite using MC-ICPMS

A minimum of 0.1 up to 0.5 g of muscovite for each sample was selected and picked under a binocular microscope. The muscovite concentrates underwent digestion in Savillex Teflon vials with HF, HNO_3 , HCl and H_3BO_3 (20 drops HF, 20 drops HNO_3 , and 10 drops HCl at 185°C, dried at 85°C; followed by 10 drops H_3BO_3

and 10 drops HCl added, left on hot plate for 5 hours at 85°C then dried at 85°C). The resulting solutions were analyzed to determine their $\delta^7\text{Li}$ values using a Thermo Finnigan Neptune MC-ICPMS. $\delta^7\text{Li}$ values are reported using the delta notation of $\delta^7\text{Li} (\text{‰}) = [({}^7\text{Li}/{}^6\text{Li})_{\text{sample}}/({}^7\text{Li}/{}^6\text{Li})_{\text{L-SVEC}} - 1] \times 1000$ relative to L-SVEC (Li-carbonate CRM - NIST 8545 (Flesch et al., 1973)).

Supplementary Figures

Figure SM1. Representative hand specimen photographs of the mantle-hosted granitoids from the Samail ophiolite.

Figure SM2. Representative sample photomicrographs of the Samail mantle-hosted granitoids.

Figure SM3. Cathodoluminescence (CL) and Backscattered electron (BSE) images of representative zircon.

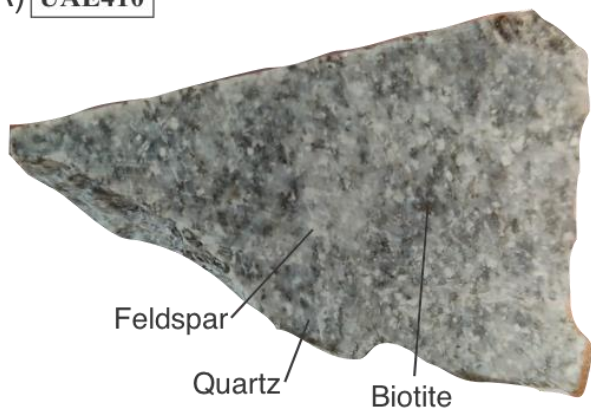
Figure SM4. REE patterns of zircon trace elements from Samail mantle-hosted granitoids and Himalaya leucogranitoids.

Figure SM5. BSE images of muscovite crystals analyzed in this study.

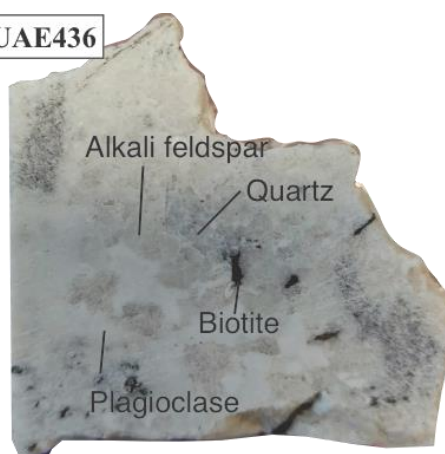
Figure SM6. MgO-TiO₂-Na₂O ternary diagram showing distribution of muscovite from Samail mantle-hosted granitoids analyzed in this study.

Figure SM7. $\delta^2\text{H}$ values for muscovite and average $\delta^{18}\text{O}$ values from quartz, zircon and whole-rock shown as frequency histograms of same samples showing values akin to metamorphic waters.

(A) UAE410



(B) UAE436



(C) MS500



(D) MS500



(E) HD



(F) HD

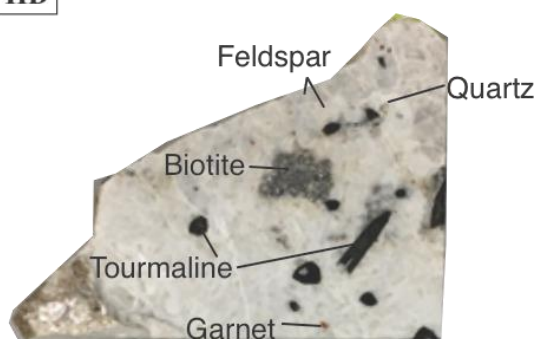


Figure SM1. Representative hand specimen photographs of the mantle-hosted granitoids from the Samail ophiolite. A) fine-grained with granular texture composed of quartz, feldspar (plagioclase and alkali feldspar) and biotite. B) coarse-grained granular texture showing alkali feldspar, plagioclase, biotite and quartz. C) medium-grained granular texture marked by quartz, feldspar, biotite, muscovite and tourmaline. D) pegmatitic granitoid with Li-rich muscovite (lepidolite). E and F) medium to coarse grained granitoid with quartz, feldspar, biotite, muscovite, and tourmaline. Black lines below each sample represent 2.5 cm.

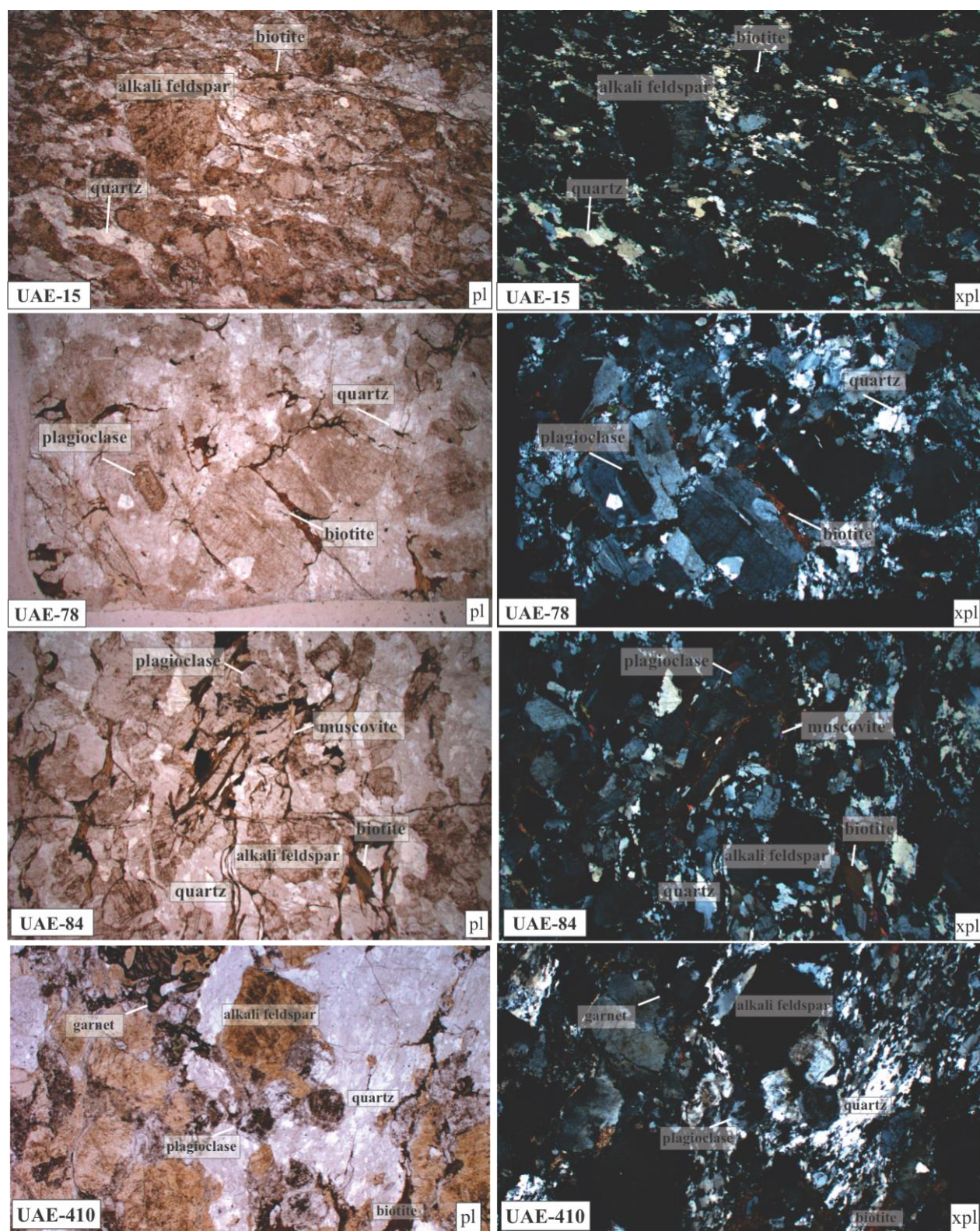


Figure SM2. Representative sample photomicrographs of the Samail mantle-hosted granitoids showing subhedral granular texture with quartz, alkali feldspar, plagioclase, biotite, muscovite and garnet. pl = plane polarized light, xpl = cross polarized light.

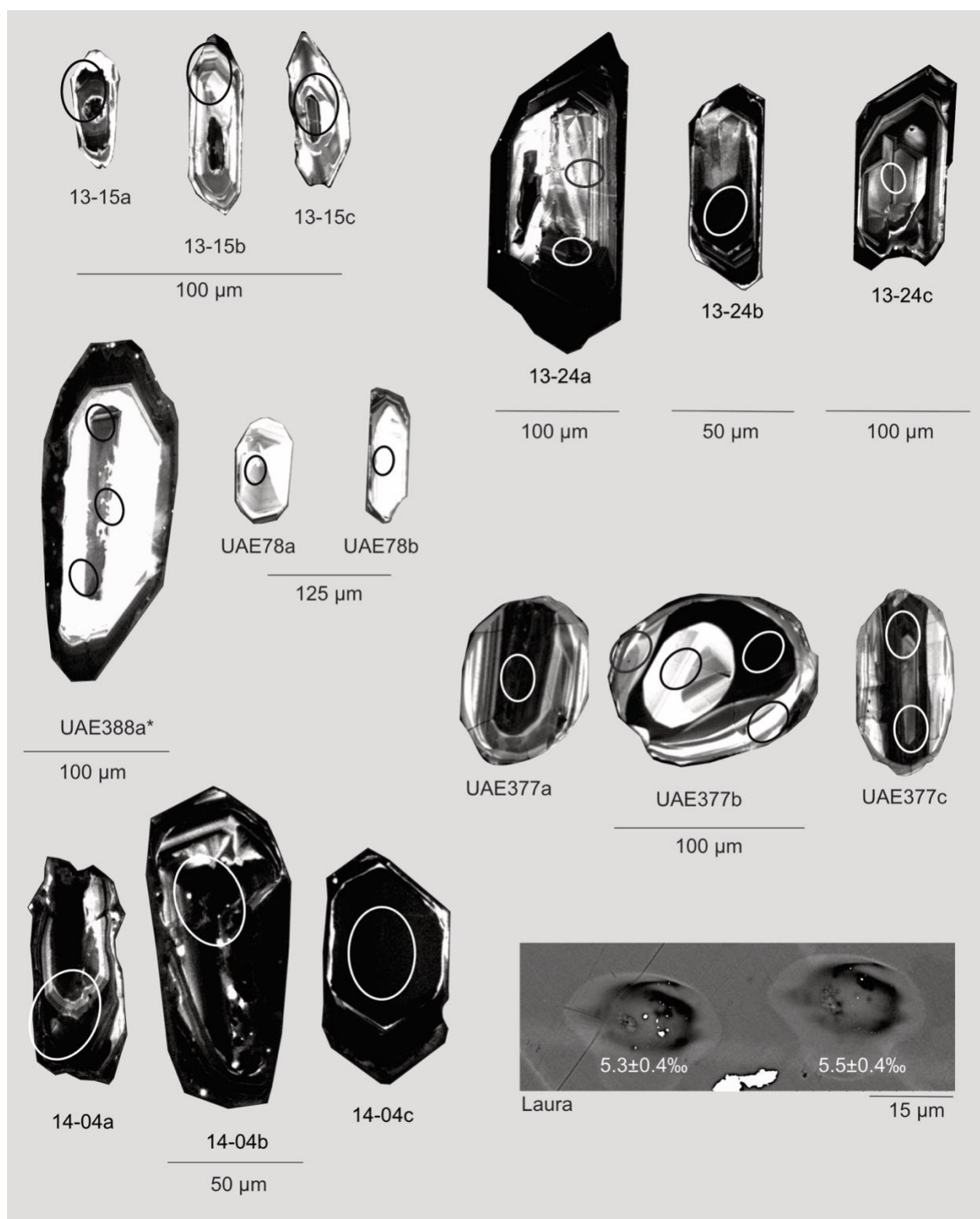


Figure SM3. Cathodoluminescence (CL) and backscattered electron (BSE) images of representative zircon from samples 13-15, 13-24, UAE377 and 14-04. Sample UAE388 data was published by Spencer et al. (2017). Spot locations are represented by black and white circles. Ion probe sputter pits are included from selected reference to illustrate the regular pit appearance (Cavosie et al., 2005).

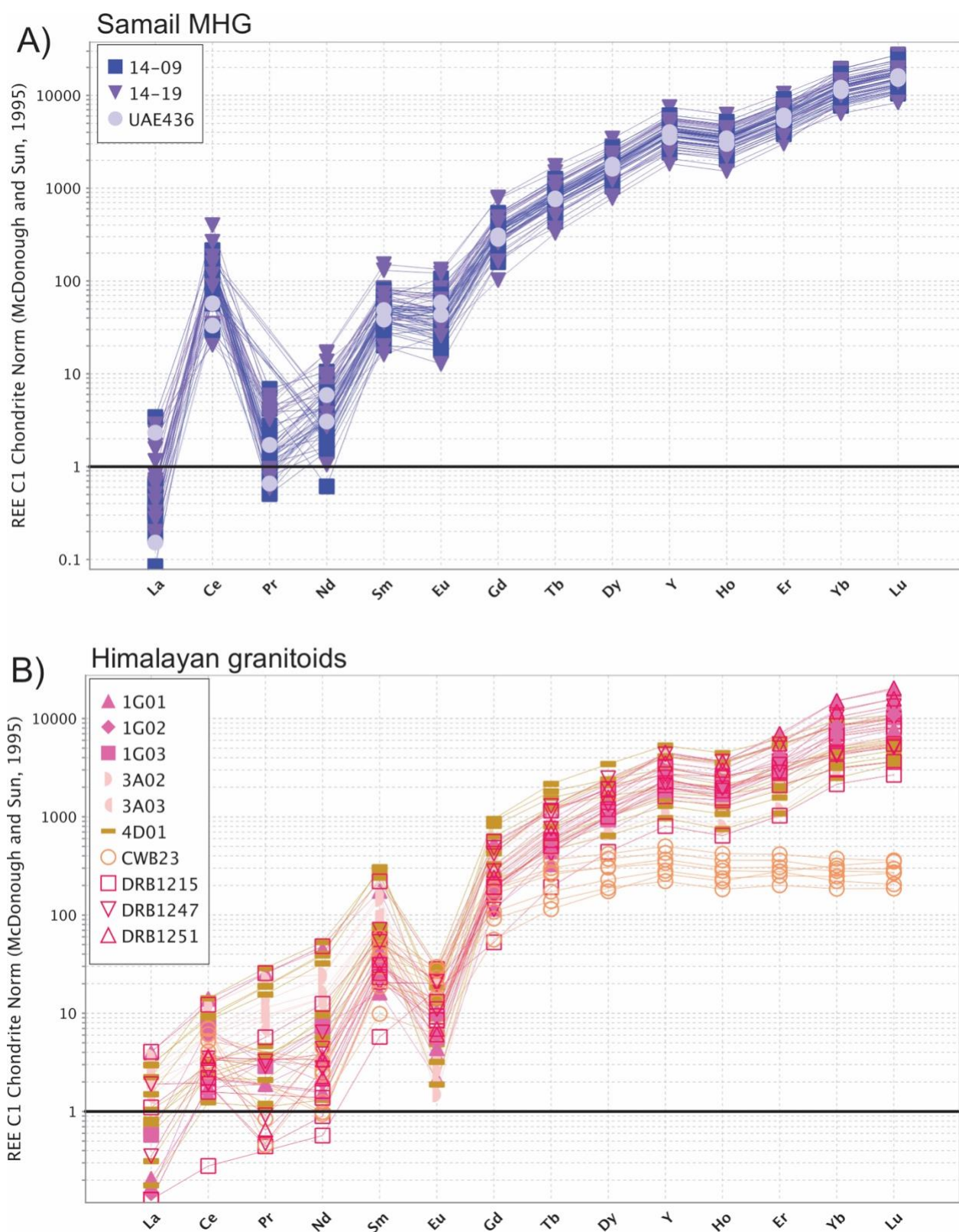


Figure SM4. REE patterns of zircon trace elements obtained in this study shown as spider diagrams of the Samail mantle-hosted granitoids (A) and Himalayan S-type granitoids (B). Chondrite normalized after Sun and McDonough (1995).

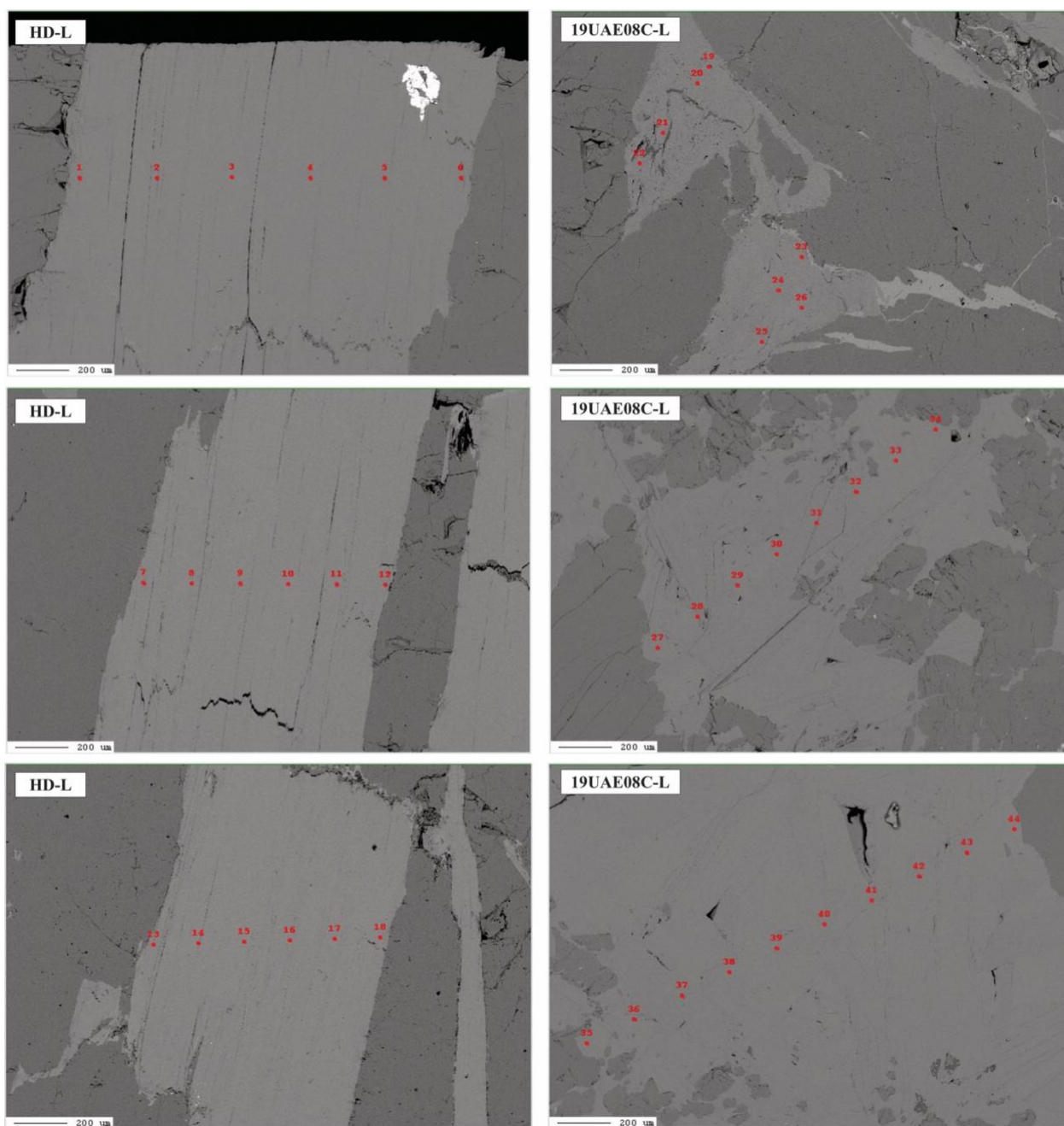


Figure SM5. BSE images of muscovite crystals from samples HD and 19UEA08C-L.

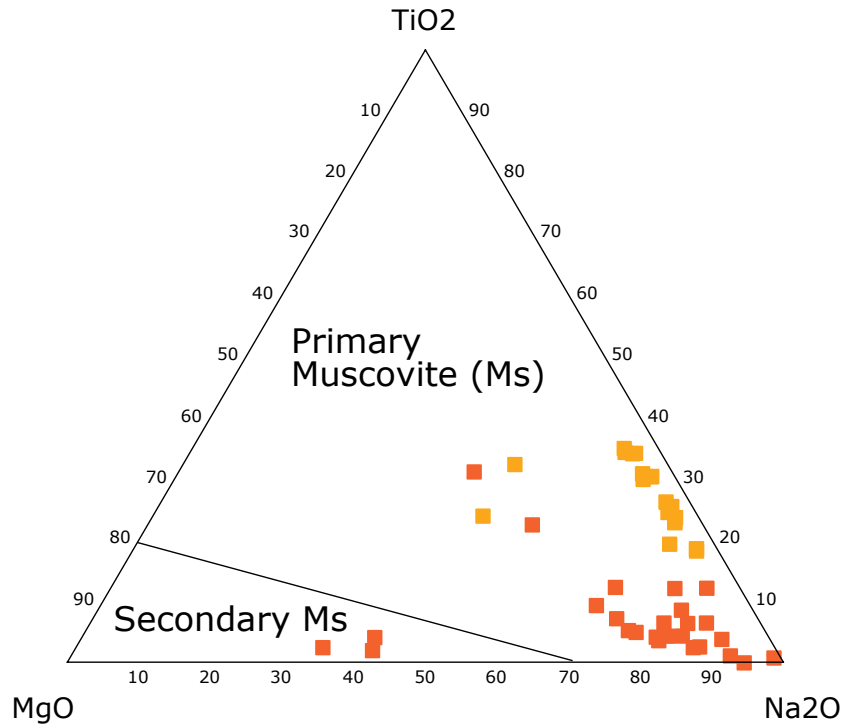


Figure SM6. MgO-TiO₂-Na₂O ternary diagram modelled after (Ballouard et al., 2016). Orange squares are HD-M and red are 19UAE08C-M.

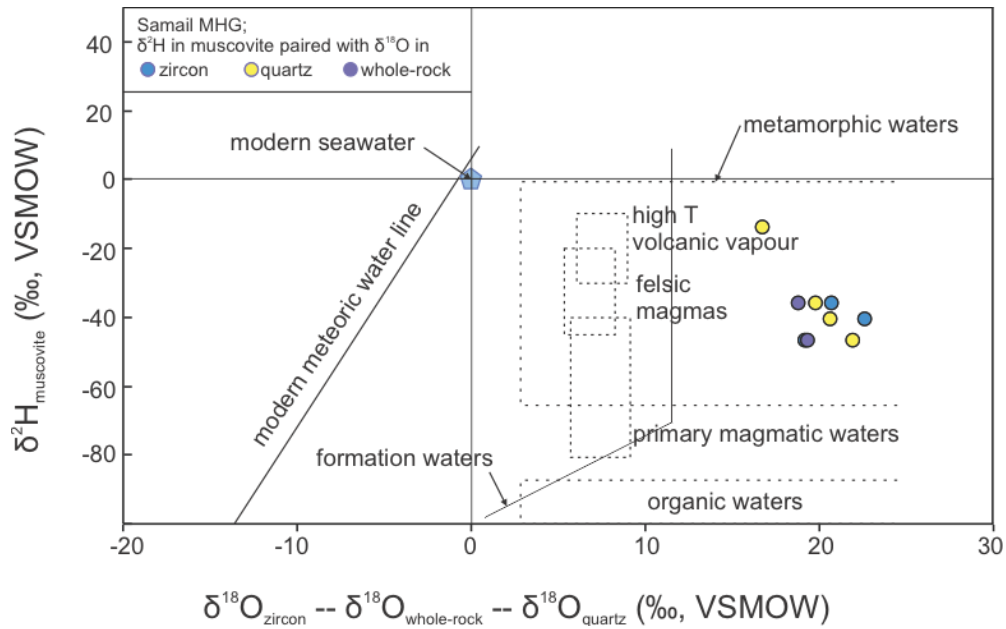


Figure SM7. Results $\delta^2\text{O}$ in muscovite paired with average $\delta^{18}\text{O}$ values in quartz, zircon and whole-rock plotting in metamorphic waters field. Data was compared to meteoric water line and water fields from Rollinson (1993).

References

- Ballouard C., Poujol M., Boulvais P., Branquet Y., Tartèse R. and Vigneresse J.-L. (2016) Nb-Ta fractionation in peraluminous granites: A marker of the magmatic-hydrothermal transition. *Geology* **44**, 231–234.
- Cavosie A. J., Valley J. W., Wilde S. A. and E.I.M.F. (2005) Magmatic $\delta^{18}\text{O}$ in 4400–3900 Ma detrital zircons: A record of the alteration and recycling of crust in the Early Archean. *Earth Planet. Sci. Lett.* **235**, 663–681.
- Rollinson H. (1993) Using geochemical data: Evaluation, presentation, interpretation: Longman Group. *Essex, Engl.*